

INVESTIGATION OF NEAR-FIELD CAVITY FLOW NOISE

Paulo Rogério Novak, paulo.novak@pucpr.br

Departamento de Engenharia Mecânica
Pontifícia Universidade Católica do Paraná
80215-901, Curitiba, PR, Brazil

Cesar J. Deschamps, deschamps@polo.ufsc.br

Samir N. Y. Gerges, samir@emc.ufsc.br

Departamento de Engenharia Mecânica
Universidade Federal de Santa Catarina
88040-900, Florianópolis, SC, Brazil

Aldo Rona, ar45@le.ac.uk

Department of Engineering
University of Leicester
Leicester LE1 7RH, UK

Abstract. *The flow past open cavities is a problem that is encountered in many engineering applications and can result in intense acoustic tones. The flow physics and acoustics of a cavity are complex and has been the subject of many studies over the years. In this paper, the tonal noise radiated by a two-dimensional cavity submerged in a turbulent flow is investigated computationally using a hybrid scheme that couples numerical flow computations with an implementation of the Ffowcs Williams – Hawkings equation. The turbulent near field is computed through Large Eddy Simulation (LES). Refined computational grids in the immediate region of the cavity and small time step are used to capture the unsteady flow physics. The unsteady characteristics of the cavity flow are discussed, together with an analysis of the main mechanisms associated with the cavity noise generation. Numerical results are presented and compared with reference solutions available in the literature.*

Keywords: *aeroacoustics, CAA, acoustic analogy*

1. INTRODUCTION

The phenomenon of flows passing over a cavity has been studied in numerous investigations in the past and has a broad range of applications, from automotive industry to aerospace applications. Earlier investigations based on full-scale aircraft have indicated that there are many sources that contribute to airframe noise, with one of them being cavity noise. For example, during the landing, there is an increase in the sound pressure level from aircraft that can be associated with the presence of a cavity created by the open landing gear (Shieh, 2000). The flow-induced cavity noise can also occur in automotive vehicles and the most relevant aerodynamic noise sources to occupants are from gaps in the doors, windows and sunroof, as well as from the air conditioning and ventilation systems.

Despite its geometric simplicity, the physics associated to flow over cavities is a complex phenomenon. For instance, the interaction of vortices with the cavity trailing edge generates a recirculating flow region in the cavity and instabilities on the shear layer, yielding both broadband and tonal noise. These tones can be originated by two mechanisms: shear layer mode and wake mode. The shear layer mode mechanism, also known as the Rossiter mechanism (Rossiter, 1964), is the most important flow-acoustic resonance in which the interaction between the free shear layer and the acoustic field produces a natural feedback loop. The wake mode, firstly noticed by Gharib and Roshko (1987), is characterized by intense oscillations due to a shedding/ejection process of vortices whose dimensions are nearly the size of the cavity, with an order of magnitude larger than that observed in the shear layer mode.

Rossiter (1964) was one of the first researchers who described the feedback mechanism, based on experimental results, and derived a semi empirical equation for the non-dimensional feedback frequencies based on a periodic phenomenon. Following Rossiter (1964), numerous studies have been devoted to cavity flows. For instance, several experimental results for the near-field flow features and cavity-wall pressure fluctuations are available in the literature (Rockwell and Naudascher, 1978; Cattafesta *et al.*, 1998; Henderson, 2000; Henderson, 2004; Grace *et al.*, 2004). An extensive data set on cavity noise has been compiled by Ahuja and Mendoza (1995) as benchmark cases for computational aeroacoustic (CAA) codes. One of the issues addressed by the authors was the effect of the cavity dimensions, the upstream boundary layer and the flow temperature on the generation of cavity noise.

From the computational point of view, computational aeroacoustics (CAA) is now becoming a common tool for predicting noise generated from flows, such as jets, airfoils and cavity flows. Recently, a number of studies about cavity flow noise have been numerically conducted by Rowley *et al.* (2002), Gloerfelt *et al.* (2001, 2003), Rubio *et al.* (2007), Ashcroft *et al.* (2001, 2003), Larchevêque *et al.* (2003) using direct numerical simulation and hybrid schemes.

In this paper, the tonal noise radiated by a two-dimensional cavity submerged in a turbulent flow is numerically investigated using a hybrid scheme that couples flow computations with an implementation of the Ffowcs Williams –

Hawkings equation. The turbulent near field is computed, in the commercial code Fluent, through Large Eddy Simulation (LES). The unsteady characteristics of the cavity flow are discussed, so as to put some light on the main mechanisms responsible for cavity noise generation. Numerical predictions are compared with reference solutions available in the literature.

2. MATHEMATICAL FORMULATION

2.1. Near Field

The near-field turbulent flow and the far-field acoustics can be described by the Navier-Stokes equations, written for a compressible and unsteady flow condition:

$$\frac{\partial \rho}{\partial t} + \frac{\partial \rho u_i}{\partial x_i} = 0 \quad (1)$$

$$\frac{\partial \rho u_i}{\partial t} + \frac{\partial \rho u_i u_j}{\partial x_j} = -\frac{\partial p}{\partial x_i} + \frac{\partial \tau_{ij}}{\partial x_j} \quad (2)$$

where the viscous stress τ_{ij} is expressed through the strain rate, S_{ij} , following the hypothesis of a Newtonian fluid:

$$\tau_{ij} = \mu S_{ij} \quad (3)$$

$$S_{ij} = \frac{\partial u_i}{\partial x_j} + \frac{\partial u_j}{\partial x_i} - \frac{2}{3} \frac{\partial u_k}{\partial x_k} \delta_{ij} \quad (4)$$

The equation for conservation of energy is also required:

$$\frac{\partial \rho E}{\partial t} + \frac{\partial \rho E u_k}{\partial x_k} = -\frac{\partial p u_k}{\partial x_k} + \frac{\partial \tau_{ij} u_j}{\partial x_i} - \frac{\partial q_k}{\partial x_k} \quad (5)$$

where E is the specific total energy, and q_k is the heat flux. The working fluid chosen for the analysis was air and, therefore, the hypothesis of ideal gas was assumed.

When Large Eddy Simulation (LES) is adopted, only the large-scale structures are explicitly computed, whereas small scales are modeled. The governing equation employed for LES are obtained by filtering the time-dependent Navier-Stokes equations in either spatial configuration. Thus, the resulting equations describe the dynamics of large eddies. Detailed description of the method may be found in Larchevêque *et al.* (2003).

The spatial average or filtering is formulated in such a way that a generic flow quantity, $\Phi(\vec{x}, t)$, is separated into the sum of a filtered component, $\overline{\Phi}(\vec{x}, t)$, and a residual, or subgrid-scale component, $\Phi'(\vec{x}, t)$:

$$\Phi(\vec{x}, t) = \overline{\Phi}(\vec{x}, t) + \Phi'(\vec{x}, t) \quad (6)$$

The filtered variable is defined by

$$\overline{\Phi}(\vec{x}, t) = \int_{V(\vec{x}, t)} G[\vec{x} - \vec{x}', \Delta(\vec{x})] \Phi(\vec{x}', t) d\vec{x}'^3 \quad (7)$$

where V is the fluid domain and $G[\vec{x} - \vec{x}', \Delta(\vec{x})]$ is the filter function that determines the scale of the resolved eddies, defined here as

$$G[\vec{x} - \vec{x}', \Delta(\vec{x})] = \begin{cases} 1/V, & \Delta(\vec{x}) \in V(\vec{x}', t) \\ 0 & \Delta(\vec{x}) \text{ otherwise} \end{cases} \quad (8)$$

with V assumed to be the volume of a computational cell.

For the compressible flow, it is convenient to use the Favre-filtering, to avoid the introduction of subgrid-scale terms into the equation of conservation of mass. Thus, the spatial filtering is rewritten as

$$\Phi(\bar{x}, t) = \tilde{\Phi}(\bar{x}, t) + \Phi''(\bar{x}, t) \quad (9)$$

with the density weighted average term being defined by

$$\tilde{\Phi}(\bar{x}, t) = \frac{\overline{\rho\Phi}(\bar{x}, t)}{\bar{\rho}} \quad (10)$$

Filtering equations (1), (2) and (5), the governing equations for the unsteady compressible Navier-Stokes equations are

$$\frac{\partial \bar{\rho}}{\partial t} + \frac{\partial(\bar{\rho} \tilde{u}_i)}{\partial x_j} = 0 \quad (11)$$

$$\frac{\partial \bar{\rho} \tilde{u}_i}{\partial t} + \frac{\partial(\bar{\rho} \tilde{u}_i \tilde{u}_j)}{\partial x_j} + \frac{\partial \bar{p}}{\partial x_i} - \frac{\partial \bar{\sigma}_{ji}}{\partial x_j} = -\frac{\partial \tau_{ji}}{\partial x_j} + \frac{\partial(\bar{\sigma}_{ji} - \tilde{\sigma}_{ji})}{\partial x_j} \quad (12)$$

$$\begin{aligned} \frac{\partial(\bar{\rho} \tilde{\varepsilon})}{\partial t} + \frac{\partial(\bar{\rho} \tilde{u}_i \tilde{\varepsilon})}{\partial x_j} + \frac{\partial \tilde{q}_j}{\partial x_j} + \bar{p} \tilde{S}_{kk} - \tilde{\sigma}_{ji} \tilde{S}_{ij} = & -\frac{\partial}{\partial x_j} \left[\bar{p} \left(u_j \varepsilon - \tilde{u}_j \tilde{\varepsilon} \right) \right] - \frac{\partial}{\partial x_j} \left[\bar{q}_j - \tilde{q}_j \right] - \\ & \left[\bar{p} \tilde{S}_{kk} - \bar{p} \tilde{S}_{kk} \right] + \left[\bar{\sigma}_{ji} \tilde{S}_{ij} - \tilde{\sigma}_{ji} \tilde{S}_{ij} \right] \end{aligned} \quad (13)$$

where \tilde{S}_{ij} is the Favre-filtered strain-rate tensor. The bar-symbol ' $\bar{\cdot}$ ' denotes a filtering operation, and the tilde-symbol ' $\tilde{\cdot}$ ' denotes a Favre filtering operation.

The subgrid-scale stresses resulting from the filtering operation are unknown and require modeling. In this work, the dynamic Smagorinsky model proposed by Germano *et al.* (1991) and Lilly (1992) was used to calculate the sub-grid scale stresses.

2.2. Far Field.

The differential form of the Ffowcs-Williams and Hawking (FW-H) equation is an exact rearrangement, with the aid of the mathematical tool of generalized functions (so-called surface distributions), of the continuity and the Navier-Stokes equations into an inhomogeneous wave equation in an unbounded space. The differential form of the FW-H equation can be written as:

$$\left(\frac{1}{c_0^2} \frac{\partial^2}{\partial t^2} - \frac{\partial^2}{\partial x_i^2} \right) [c_0^2(\rho')] = \frac{\partial}{\partial t_i} [\rho_0 U_n \delta(f)] - \frac{\partial}{\partial x_i} [F_i \delta(f)] + \frac{\partial^2 (HT_{ij})}{\partial x_i \partial x_j} \quad (14)$$

$$U_n = \left[\frac{\rho u_i}{\rho_0} + \left(1 - \frac{\rho}{\rho_0} \right) v_i \right] n_i \quad F_i = [(p') \delta_{ij} - \tau_{ij} + \rho u_i (u_j - v_j)] n_j$$

$$T_{ij} = \rho u_i u_j + [(p - p_0) - c_0^2(\rho - \rho_0)] \delta_{ij} - \tau_{ij} \text{ (so-called Lighthill's stress)}$$

The right-hand side of Eq. (14) is formed by three source terms. The first one corresponds to a monopole distribution (thickness noise) due to the geometry and the kinematics of moving solid bodies. The second source term is a dipole distribution (loading noise) generated by the interaction of the flow field with solid boundaries. Finally, the third term is a quadrupole source distribution, accounting for nonlinear effects, generated by shocks, turbulence and vorticity in the flow field.

If the wave solution of the differential form of the FW-H equation, Eq. (14), is written by using the free space Green's function, the integral form of the FW-H equation can be derived. Thus, Eq (14) can be written as

$$4\pi Hp'(\vec{x}, t) = \frac{\partial^2}{\partial x_i \partial x_j} \int_V \left[\frac{T_{ij}}{r|1-M_r|} \right]_{\tau=t-\frac{r}{c_0}} dV(\vec{y}) - \frac{\partial}{\partial x_i} \int_S \left[\frac{F_i}{r|1-M_r|} \right]_{\tau=t-\frac{r}{c_0}} dS(\vec{y}) + \frac{\partial}{\partial t} \int_S \left[\frac{U_n}{r|1-M_r|} \right]_{\tau=t-\frac{r}{c_0}} dS(\vec{y}) \quad (15)$$

$$M_r = v_i r_i / c_0$$

where $|1-M_r|^{-1}$ is the Doppler factor, v_i is the local velocity component on the control surface and r_i is the component of the vector position between the observation and source locations.

3. PROBLEM DESCRIPTION.

The cavity considered in the present study represents an automobile door cavity (Fig. 1a) presented at the Third Computational Aeroacoustic Workshop on Benchmark Problems (Henderson, 2000). This cavity was previously considered in flow simulations carried out through DNS - Direct Numerical Simulation (Kurbatskii and Tam, 2000), DES - Detached Eddy Simulation (Shieh *et al.*, 2000) and U-RANS - Unsteady Reynolds Averaged Navier-Stokes (Ashcroft *et al.*, 2003).

A two-dimensional rectangular enclosure of length $L=15.9\text{mm}$ and depth $D=24.7\text{mm}$ is cut into a flat plate. There is a 3.3mm thick partial cover, or lip, over the upstream portion of the cavity that reduces the cavity opening to 8.76mm in the streamwise direction. A fully turbulent boundary layer, with a 1/7th power law profile, approaches the cavity. The boundary layer thickness is 17mm and the free stream Mach number is 0.147.

The flow over the cavity is taken as two-dimensional and the domain is discretized by using a structured rectangular mesh. Time-resolved flow predictions are obtained using a compressible turbulence closure scheme for LES, available in the commercial code Fluent. The Roe-FDS second order accurate upwind interpolation scheme is used to estimate fluxes of flow properties at each control volume resulted from the domain discretization. The governing equations are integrated using an implicit density based solver.

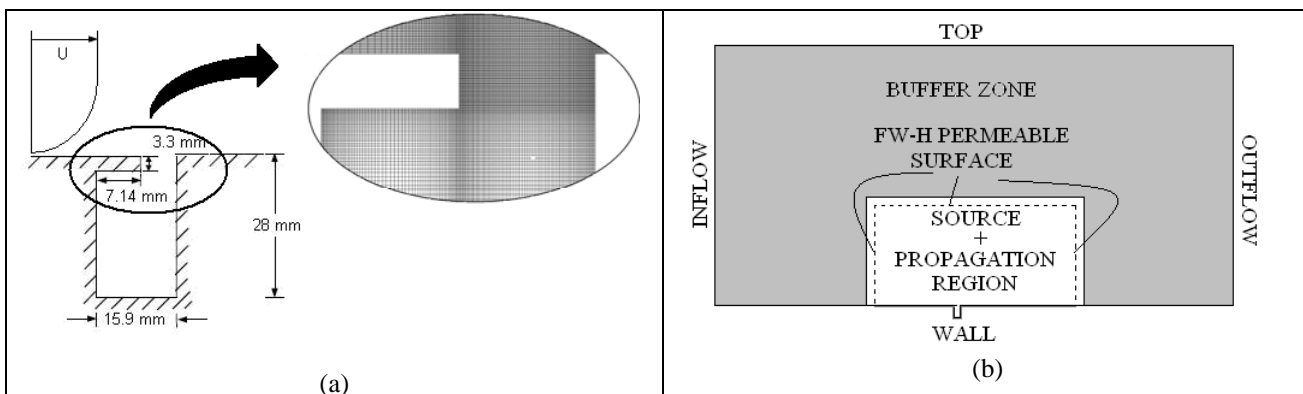


Figure 1. (a) Cavity geometry and computational mesh used in the present study; corresponding to the problem of category 6. (Kurbatskii and Tam, 2000); (b) Computational domain.

3.1. The computational domain and numerical boundary condition

Figure 1b shows the two dimensional computational domain for both the source and propagation region. With the origin of the coordinate system situated at the left boundary. The computational domain for LES (excluding the buffer zones) for this cavity extend from $20 \leq x/D \leq 43.77$ in the streamwise direction and $-1 \leq y/D \leq 11.88$ in the normal direction. At the outflow, pressure outlet with non-reflecting boundary condition was applied to enable the acoustic waves and unsteady flow structures to propagate out of the domain without causing significant numerical reflections. At the top, a symmetry boundary condition was imposed. At the inflow, velocity components were fixed to describe the approaching turbulent boundary layer profile, so as to ensure the correct boundary layer on the leading edge of the cavity. The velocity profile utilized was the one-seventh power law velocity profile. In order to obtain the correct boundary layer thickness at the cavity lip, the slip condition was assumed for a small section of the upstream wall. For all the remaining walls a non slip boundary condition was considered. To minimize reflection of acoustic waves and vertical structures at the boundaries, a buffer zone was added to the computational domain with a length of $20D$ in both directions. Finally, all walls were assumed to be adiabatic.

3.2. Computational grid: Near and Far Field

The LES mesh is refined near to solid walls and in the region of the shear layer. The mesh is also progressively stretched towards the outlet region to help dissipating vertical structures before they reach the outlet boundary, but observing a maximum stretching of 10%. Due to the fact that second order schemes are used for the LES, the mesh size need to be small enough to avoid excessive dispersion and dissipation errors that could contaminate the acoustic field prediction.

The frequency and amplitude pressure results was compared with three grid levels. The first, second and third mesh had a total of 229.000, 300.000 and 364.000 cells, respectively. For the first mesh, the difference in the first frequency on the second and third mesh was approximately 12%, and in the amplitude was 7 dB. For the second mesh, the amplitude, reference to first frequency, was the same, and the difference in the amplitude, reference to second frequency, was around 8 dB. From this we conclude that the grid with 364.000 cells is sufficient for resolving the flow field.

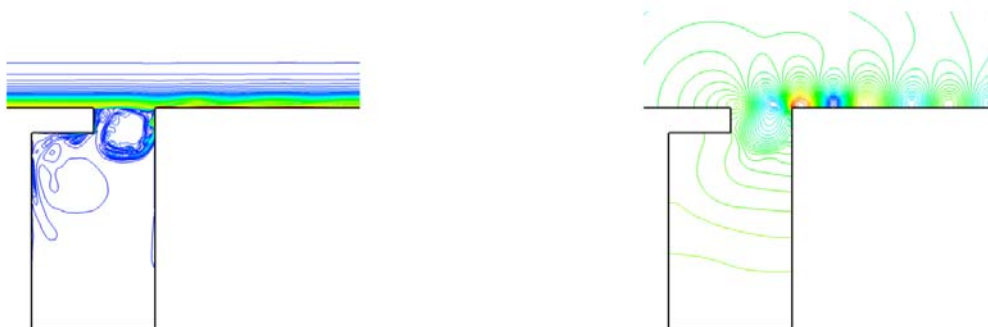
The mesh had a total of 364.000 cells of approximate size equal to $0.0017D$, with $y^+ \approx 1$ being sought near the solid walls. The dynamic Smagorinsky subgrid scale model was used to estimate the contribution of unresolved scales on the flow field. The simulations were started from an initial solution provided by steady state RANS k-epsilon simulation and carried out until a statistically steady state was reached.

The acoustic calculations were carried out by the FW-H acoustic analogy, with impenetrable and permeable surfaces. The source region for the impenetrable surface corresponds to the solid surface of the cavity, spanning from $21D$ to $42.7D$ in the streamwise direction. The permeable surface extends itself from 0 to $10.8D$ in the normal direction and from $21D$ to $42.7D$ in the streamwise direction. This surface control is slightly smaller than the total domain used to solve the LES, in order to minimize the effect of boundary conditions on the fluctuating variables inside the flow domain.

4. RESULTS AND DISCUSSIONS

4.1. Near Field

Figure 2 shows results for vorticity and pressure contours at four different time instants, corresponding to second Rossiter mode, which is dominant for this flow geometry. Figure 2(a) illustrates the growth of a vortex, which is separated by growth of instabilities in the shear layer. The vortical structure impinges on the trailing edge of the cavity, as indicated in Fig. 2(b), and part of its structure is convected downstream, forming smaller vortices along the flat plate (Fig. 2(c)). The presence of such convected vortices can be clearly detected in the pressure contour plot. Part of the vortical motion is transferred to the cavity, creating a large recirculation region of small vortices (Fig. 2(d)), which cause instabilities on the shear layer. The vorticity contours also show a steady vortex at the neck of the cavity, which is an evidence that the interaction between the shear layer and the flow inside the cavity is very weak for this oscillation mode.



(a)

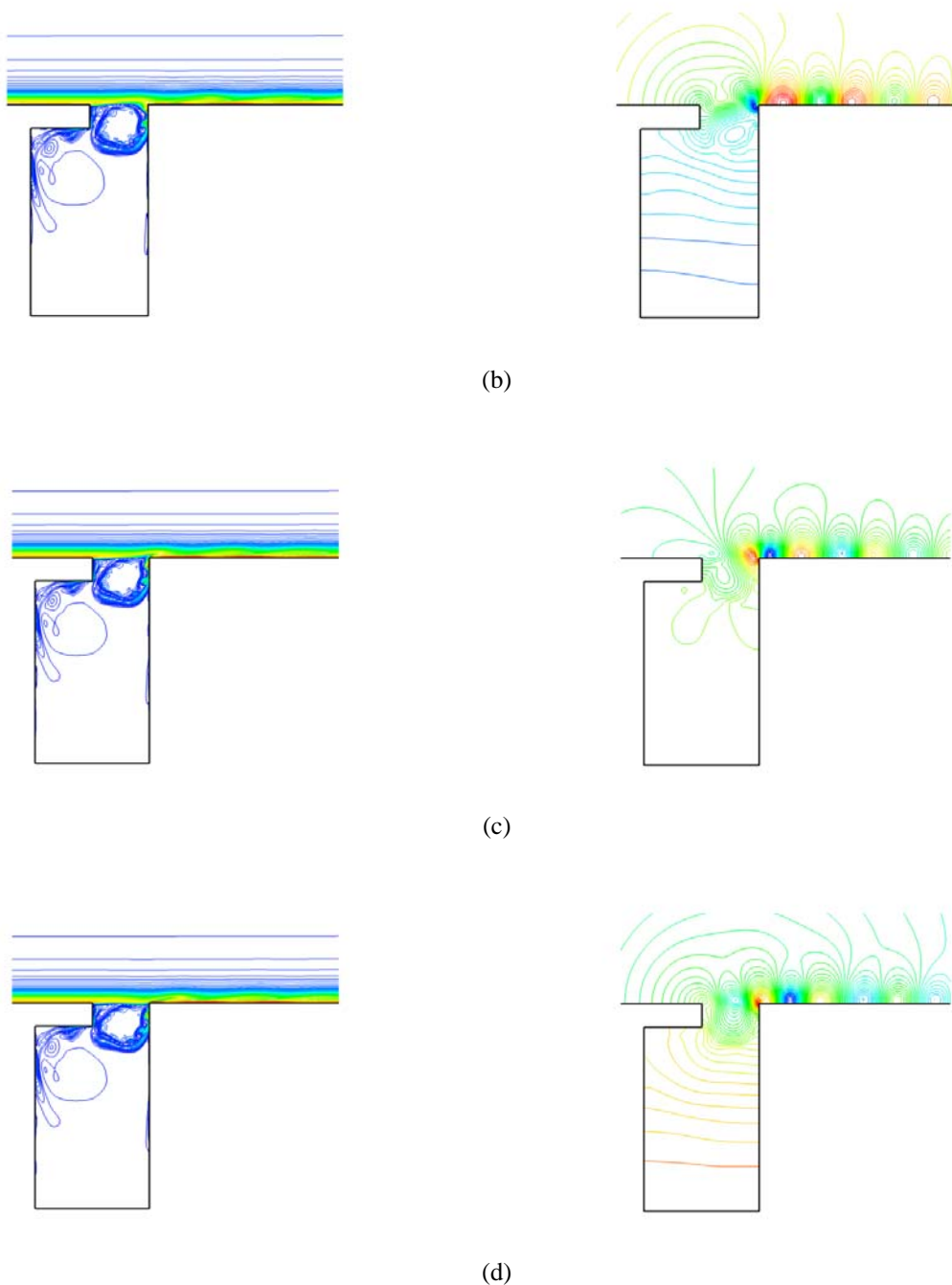


Figure 2. Vorticity contours (on the left) and pressure contours (on the right) during one cycle of oscillation for the shear layer mode (second Rossiter mode) at different time instants.

Figure 3 shows the spectrogram of the pressure signal at the centre of the left wall of the cavity, which was obtained by using 2,048 points FFT's, with a flat top window and 50% overlap. The observed dominant peak at 1,809 Hz corresponds to the characteristic frequency indicated by the classic theory for Helmholtz resonators ($f = 1,850$ Hz). The secondary peak at 3,618 Hz is the first harmonic of the dominant tone at 1,809 Hz.

In order to identify the oscillation frequencies, time signal of pressure have been recorded at three points in the cavity: the centre of the left wall, the centre of the cavity floor and the centre of the right wall. Figure 4 (a) shows the time history and Sound Pressure Level at the centre of the left wall after the flow reached a statically steady regime.

Figure 4(b) indicates that the dominant frequency occurs at a Strouhal number of 0.573 (1,809Hz). This is in good agreement with the value of 0.551 predicted by Rossiter equation for the second shear layer mode, with a ratio between the convection velocity of vortices and the free-stream velocity of 0.33, suggested by Henderson (2004), and a factor of 0.25 to account for the lag time between the impact of a structure on the downstream corner and the emission of an acoustic wave, as suggested by Rossiter (1964).

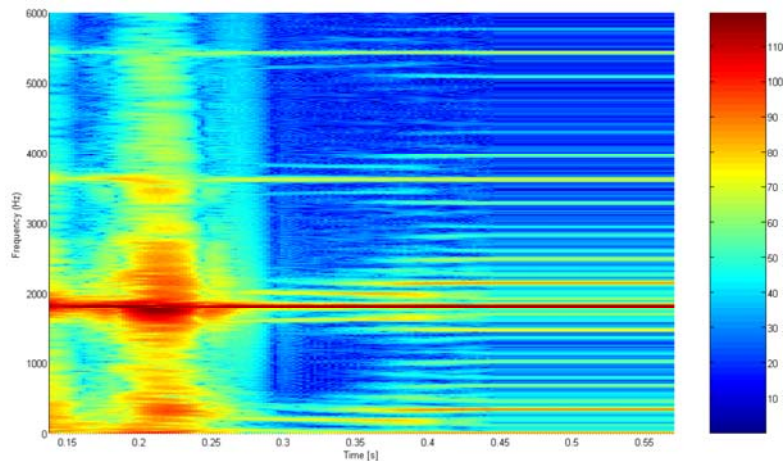


Figure 3. Spectrogram of the pressure signal at the centre of the left wall of the cavity .

As shown in Table 1, the results are also in good agreement with the experimental data obtained by Henderson (2000, 2004) and with numerical results found by other authors. However, it should be said that results for frequency and amplitude are very sensitive to boundary layer thickness at the cavity mouth.

Table 1. Comparison between prediction of the present study and results from other authors (bold numbers represent the dominant frequency).

	Authors	δ (mm)	Frequency [Hz]	Amplitude [dB]
Experimental	Henderson (2000)	2	1824	144
			3648	111
		12	1824	134
			2016	113
	Henderson (2004)	14	2848	106
			3552	111
			1727.3	124
		17	3136.4	106
			3568.2	101
			1624	116.5
Numerical	Ashcroft et al. (2000)	22	1960	141
			3920	111
	Ashcroft et al. (2003)	18.44	1850	127
	Moon et al. (2000,2003)	19	2080	133
	Shieh et al. (2000)	1.5	1852.61	146
			3705.22	107
	Kurbatsii et al. (2000)	1	5557.82	99
		2	2200	106
		3	1990	124
	Lin et al. (2004)	14	1840	110
			1381	107
			2880	104
	Zhang et al (2004)	12	5662	91
Ahn et al (2008)	2.9	1890	137.1	
Present study	17	1976.1	143.87	
		1809.3	128.9	
		3618.6	100.44	

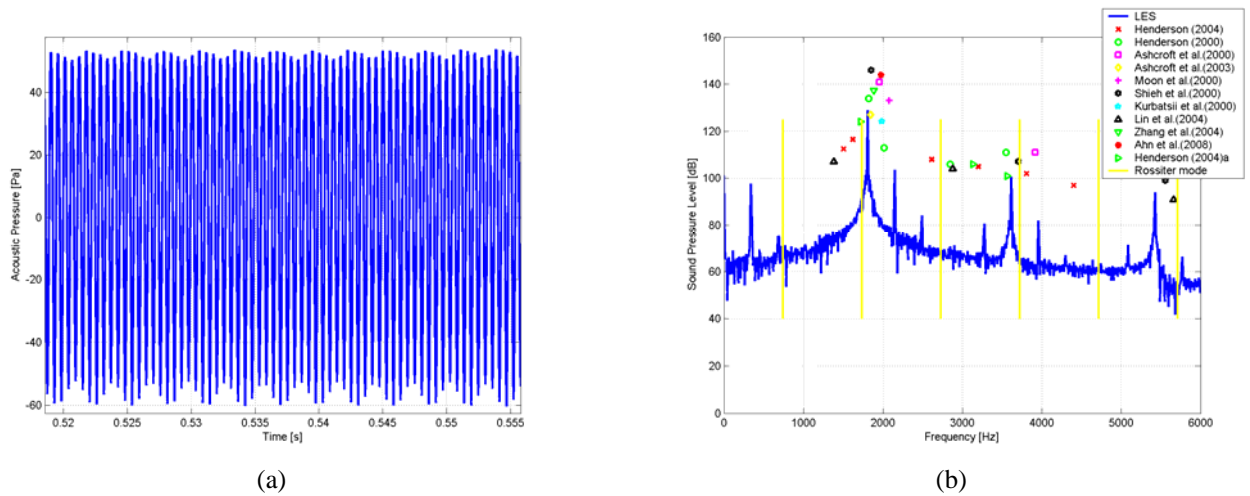


Figure 4. (a) Time signal and (b) noise spectrum at the centre of the left wall of the cavity (location: 29.58D,-0.55D).

4.2 Far-field Results.

Contours for far field pressure in Figures 5 show the directivity of the acoustic field propagated away from the cavity which is characteristic of a monopole acoustic source in low subsonic flow stream. This predominance of a monopole noise source is in agreement with results of Ashcroft *et al.* (2003), Shieh *et al.* (2000) and Kurbatskii *et al.* (2000).

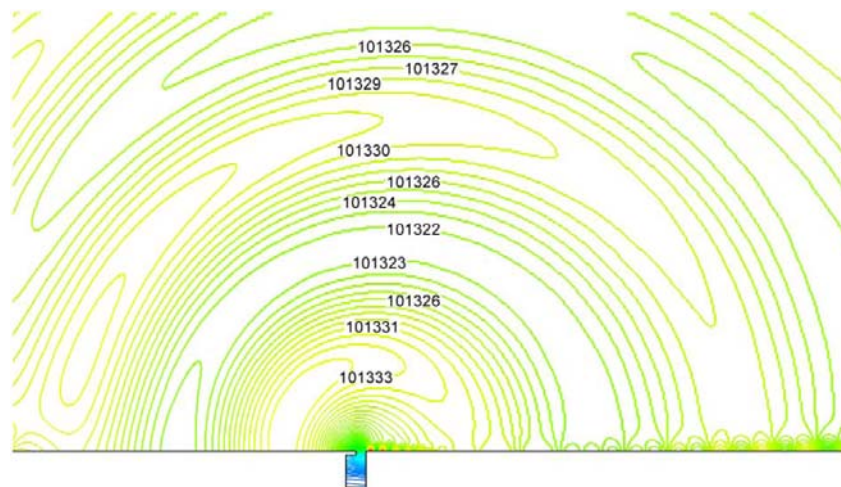


Figure 5. Far field pressure contours lines showing a monopole acoustic field.

The time history of acoustic pressure and the noise spectrum, using Ffowcs Williams and Hawkings acoustic analogy, are shown in Figs. 6 and 7, respectively, for an observer located 2,0m directly above the cavity mouth. Sound Pressure Level results for the first peak frequency (~90dB) at far-field are in agreement with results obtained by Ashcroft *et al.* (2003).

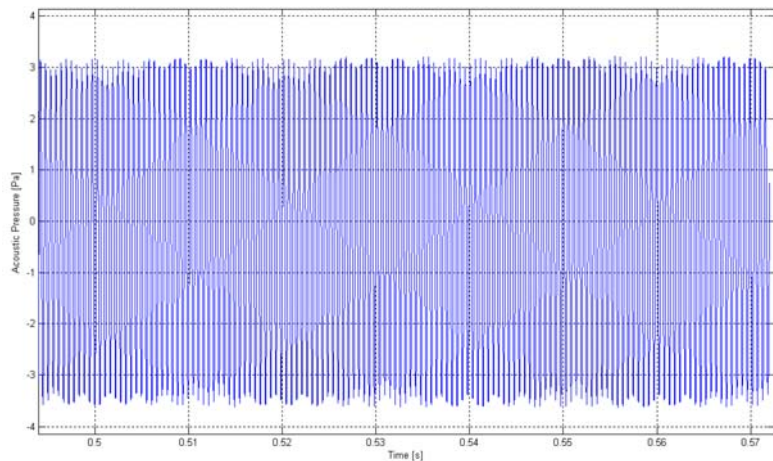


Figure 6. Time history of acoustic pressure at far field.

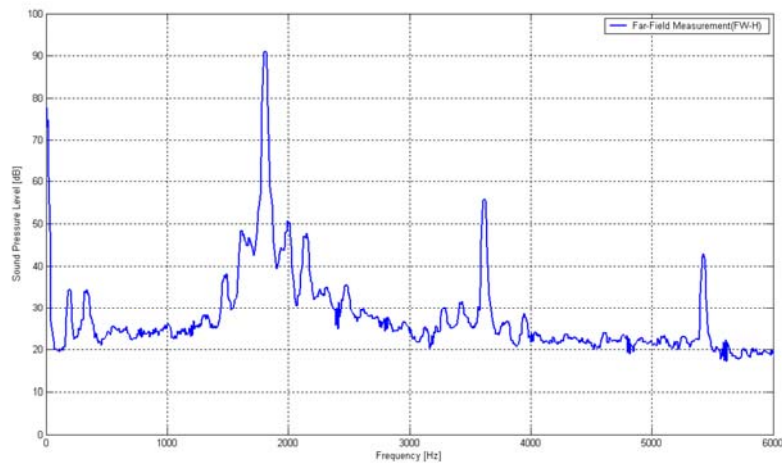


Figure 7. Noise spectrum at far field.

5. CONCLUSIONS

This paper reports a study in which a hybrid CAA approach was used to predict acoustic noise generated by turbulent flow over an automobile door cavity. The flow in the source region was computed using LES and then coupled to the Ffowcs Williams and Hawkins acoustic analogy. Grid refinement was observed in the immediate region of the cavity and small time step were used to properly capture flow unsteadiness. Good agreement was observed between the results obtained in the present study and experimental and numerical results available in the literature. Resonance frequencies and sound pressure levels are predicted accurately in the acoustic near-field and far-field. It has also been noticed that the prediction is very sensitive to some parameters of the numerical simulation, such as the boundary layer thickness at the inlet, grid refinement and size of the computational domain.

6. ACKNOWLEDGEMENTS

The authors thank CNPq (Brazilian Research Council) for supporting the present study.

7. REFERENCES

- Ahuja, KK, Mendoza, J., (1995). "Effects of cavity dimensions, boundary layer and temperature on cavity noise with emphasis on benchmark data to validate computational aeroacoustic codes". NASA Technical Report N95-24879.
- Ahn H., Lien F., Larsson J., and Hines J. (2008). "International Journal of Computational Fluid Dynamics". Vol. 22, Nº 1-2, 39-47.
- Ashcroft, G.B., Takeda, K. and Zhang, X. (2000) " Computations of Self-Induced oscillatory flow in an automobile door cavity". Proceedings of Third Computational Aeroacoustics Workshop on Benchmark Problems, p. 355–361.
- Ashcroft, G.B. and Zhang, X. (2001) "A computational investigation of the noise radiated by flow-induced cavity oscillations", AIAA Paper 2001 -0512.

- Ashcroft, G.B., Takeda, K. and Zhang, X. (2003) "A numerical investigation of the noise radiated by a turbulent flow over a cavity", *Journal of Sound and Vibration* 265(1), 43-60.
- Cattafesta L. N., Garg S., Kegerise M. A., Jones G. S. (1998). "Experiments on Compressible Flow-Induced Cavity Oscillations". AIAA Paper 98-2912.
- Gharib, M. and A. Roshko (1987). The Effect of Flow Oscillations on Cavity Drag. *Journal of Fluid Mech.*, 501–530.
- Grace S.M., Dewar W. G., Wroblewski D. E. (2004). "Experimental investigation of the flow characteristics within a shallow wall cavity for both laminar and turbulent upstream boundary layers". *Experiments in Fluids* (36) 791–804.
- Germano M., Piomelli U., Moin P., and Cabot W. H., (1991) "A dynamic subgrid-scale eddy viscosity model," *Physics Fluids A* 3, 1760.
- Gloerfelt, X., Bailly, C., Juvé, D. (2003) "Direct computation of the noise radiated by a subsonic cavity flow and application of integral methods". *Journal Sound and Vibration*, v. 266, p. 119–146.
- Gloerfelt, X., C. Baill, and D. Juve (2001). "Direct Calculation of Cavity Noise and Validation of Acoustic Analogies". In *Proceedings of NATO/RTO Applied Vehicle Technology Panel, Symposium on Aging Mechanisms and Control, Development in Computational Aero- and Hydro-Acoustics*, Manchester, UK. Karamcheti, K. (1955). "Acoustic radiation from two-dimensional rectangular cutouts in aerodynamic surfaces". Tech. Note 3487, N.A.C.A.
- Henderson, B. (2000) "Automobile noise involving feedback - sound generation by low speed cavity flows". *Proceedings of Third Computational Aeroacoustics Workshop on Benchmark Problems*, p. 95–100.
- Henderson, B. (2004) "Sound Generation in Viscous Problems - Sound Generation by flow over a cavity". *Proceedings of Fourth Computational Aeroacoustics Workshop on Benchmark Problems*, p. 71–77.
- Kurbatskii, K. K.; Tam, C. K. W. (2000) "Direct numerical simulation of automobile cavity tones". *Proceedings of Third Computational Aeroacoustics Workshop on Benchmark Problems*, p. 371–383.
- Lai, H., Luo, K. H., (2007). "A three-Dimensional Hybrid LES-Acoustic Analogy Method for Predicting Open- Cavity Noise". *Flow Turbulence Combust* 79, 59-82.
- Larchevêque L., Sagaut P., Mary I., and Labbe O., and Comte P. (2003). "Large-eddy simulation of a compressible flow past a deep cavity" *physics of fluids*, vol. 15, number 1.
- Lighthill, M. J. (1952) "On sound generated aerodynamically i: General theory". *Philosophical Transactions of the Royal Society, Série A*, v. 211, p. 564–587, 1952.
- Lighthill, M. J. (1954) "On sound generated aerodynamically ii: Turbulence as a source of sound". *Philosophical Transactions of the Royal Society, Série A*, v. 222, p. 1–32, 1954.
- Lin, Wen H. and Loh, Roy H. (2004) "Numerical solutions to the fourth and second computational aeroacoustics (CAA) workshop benchmark problems"; *Proceeding Fourth Computational Aeroacoustics (CAA) Workshop on Benchmark Problems*, p. 187-196.
- Lilly D. K., (1992) "A proposed modification of the Germano subgrid-scale closure method," *Phys. Fluids A* 4, 633.
- Moon, Y. J., Koh, S. R., Cho, Y., and Chung, J. M. (2000). "Aeroacoustic computations of the unsteady flows over a rectangular cavity with a lip". *Proceedings of Third Computational Aeroacoustics Workshop on Benchmark Problems*, p. 347–353.
- Rossiter J. E. (1964). "Wind-tunnel experiments on the flow over rectangular cavities at subsonic and transonic speeds". *Reports and Memoranda* 3438, Aeronautical Research Council.
- Rowley, C. W.; Colonius, T.; Basus, A. J. (2002). On self-sustained oscillations in two-dimensional compressible flow over rectangular cavities. *Journal Fluid Mechanics*, v. 455, p. 315–346.
- Rockwell, D. and E. Naudascher (1978). "Review – Self-Sustained Oscillations of Flow Past Cavities". *Journal of Fluids Engineering* 100, 152–165.
- Rubio G., De Roeck W., Baelmans M. and Desmet W. (2007). "Numerical Identification of Flow-Induced Oscillation Modes in Rectangular Cavities using Large Eddy Simulation". *International Journal for Numerical Methods in Fluids*, Vol. 53(5), pp. 851-866.
- Shieh, C. M.; Morris, P. J. (2000). "A parallel numerical simulation of automobile noise involving feedback". *Proceedings of Third Computational Aeroacoustics Workshop on Benchmark Problems*, p. 363–370.
- Zhang, Z.; Barron, R. C.; An, F. (2004) "Spectral analysis for air flow over a cavity"; *Proceeding Fourth Computational Aeroacoustics (CAA) Workshop on Benchmark Problems*, p. 197-204.
- Williams, J. E. F.; Hawkings, D. L. (1969) "Sound generation by turbulence and surfaces in arbitrary motion". *Proceedings Royal Society London Series A: Mathematical and Physical Sciences*, v. 264, p. 321–342, 1969.

8. RESPONSIBILITY NOTICE

The authors are the only responsible for the printed material included in this paper.